ARMY RESEARCH LABORATORY

Preliminary Study of Coupling Electromagnetic Energy to Primasheet-1000 Explosive

by Thuvan Piehler, Charles Hummer, Richard Benjamin, Kevin McNesby, Eugene Summer, and Vincent Boyle

ARL-TR-6446 **May 2013**

NOTICES

Disclaimers

The findings in this report are not to be construed as an official Department of the Army position unless so designated by other authorized documents.

Citation of manufacturer's or trade names does not constitute an official endorsement or approval of the use thereof.

Destroy this report when it is no longer needed. Do not return it to the originator.

Army Research Laboratory
Aberdeen Proving Ground, MD 21005-5066

ARL-TR-6446 **May 2013**

Preliminary Study of Coupling Electromagnetic Energy to Primasheet-1000 Explosive

Thuvan Piehler, Charles Hummer, Richard Benjamin, Kevin McNesby, Eugene Summer, and Vincent Boyle
Weapons and Materials Research Directorate, ARL

REPORT DOCUMENTATION PAGE	Form Approved OMB No. 0704-0188

1. REPORT DATE *(DD-MM-YYYY)*	2. REPORT TYPE	3. DATES COVERED (From - To)
May 2013	Final	1 October 2009–31 January 2012

4. TITLE AND SUBTITLE
Preliminary Study of Coupling Electromagnetic Energy to Primasheet-1000 Explosive

5a. CONTRACT NUMBER

5b. GRANT NUMBER

5c. PROGRAM ELEMENT NUMBER

6. AUTHOR(S)
Thuvan Piehler, Charles Hummer, Richard Benjamin, Kevin McNesby, Eugene Summer, and Vincent Boyle

5d. PROJECT NUMBER
FPST04

5e. TASK NUMBER

5f. WORK UNIT NUMBER

7. PERFORMING ORGANIZATION NAME(S) AND ADDRESS(ES)
U.S. Army Research Laboratory
ATTN: RDRL-WML-C
Aberdeen Proving Ground, MD 21005-5066

8. PERFORMING ORGANIZATION REPORT NUMBER
ARL-TR-6446

9. SPONSORING/MONITORING AGENCY NAME(S) AND ADDRESS(ES)

10. SPONSOR/MONITOR'S ACRONYM(S)

11. SPONSOR/MONITOR'S REPORT NUMBER(S)

12. DISTRIBUTION/AVAILABILITY STATEMENT
Approved for public release; distribution is unlimited.

13. SUPPLEMENTARY NOTES

14. ABSTRACT
It is anticipated that the introduction of high currents will increase the energy content of the combustion gases in the vicinity of the detonation front through ohmic heating. This increased energy should then lead to an increase in the detonation velocity. The approach is to transfer the stored electrical energy from a 160-kJ (5.5-kV) capacitor bank into the conductive zone behind the detonation front of an explosive reaction. The power supply employs a 6.5-kV, 0.010-F, 200-kJ capacitor bank. The explosive portion of the experimental apparatus consists of two copper plates (2.54 cm wide × 50 cm long × 1.27 cm thick) separated by a 0.1-, 0.2-, or 0.3-cm layer of Primasheet-1000 explosive. Upon initiation of the Primasheet-1000 explosive, an explosive switch allows the energy stored in the pulsed power assembly to be transferred through the copper plates and into the conducting reaction zone of the detonation front. Advanced diagnostics are used to image the advancing detonation front and to measure detonation velocity. Initial results show that there was an increase of ~4.2% in the detonation velocity observed in 0.1-cm-thick layers and ~2.6% enhancement in 0.2-cm-thick layers of Primasheet-1000 while inputting the electric energy into the reaction zone. No detonation velocity enhancement was observed in 0.3-cm-thick layers of Primasheet-1000 explosive.

15. SUBJECT TERMS
sheet explosive, electromagnetic, coupling energy, detonation velocity, electrical energy coupling, Primasheet-1000

16. SECURITY CLASSIFICATION OF:			17. LIMITATION OF ABSTRACT	18. NUMBER OF PAGES	19a. NAME OF RESPONSIBLE PERSON
a. REPORT	b. ABSTRACT	c. THIS PAGE			Thuvan Piehler
Unclassified	Unclassified	Unclassified	UU	32	19b. TELEPHONE NUMBER (*Include area code*) 410-278-0319

Standard Form 298 (Rev. 8/98)
Prescribed by ANSI Std. Z39.18

Contents

List of Figures

List of Tables

Acknowledgments

The U.S. Army Research Laboratory, Weapons and Materials Research Directorate, Protection Division, Energetic Technology Branch, Applied Physics Branch funded this effort through the Electromagnetic Coupling with Explosive Program.

Deborah Pilarski, William Sickles, Ray Sparks, and Ronnie Thompson assisted in the experiments.

Scott Crespi, Ensign-Bickford Aerospace and Defense Company, provided Primasheet-1000 explosive for testing.

Dr. Andrew Porwitzky provided critical technical review of the technical report.

1. Introduction

Typically, about two-thirds of the chemical energy stored in the high explosive is transferred kinetically through fragmentation effects. Significant amounts of energy are typically wasted in fragmentation, with usually only about 15%–20% transferred to the target (*1*). The fragmentation process absorbs a portion of the explosive energy and decreases the energy available to generate blast (*2*). To enhance blast effects, the total explosive yield must be increased. There are two mechanisms that lead to an enhanced detonation and supplement the chemical energy release within the wave front: energy addition prior to the reaction zone, and a modification of the dynamics of the detonation products, called overdriven detonation. It is possible to influence the detonation front by adding an external energy source to the chemical energy of the explosives. An external energy source such as electrical energy can influence the propagation characteristics of a detonation (*3*). If electrical energy could be coupled into the explosive detonation wave by passing electric current through it, a significant fraction of the chemical energy should be converted to electromagnetic energy.

Tasker (*4*) has stated that the reaction zone between the shock front and the Chapman-Jouguet plane (C-J plane) of a detonating explosive is an electrical conductor. The gaseous detonation products and the unreacted explosive are insulators. If an electric field E applies to a high explosive, then current flows only in the reaction zone, which is less than 0.1 mm wide; the subsequent electrical power P_{elec} deposited per unit area in the high explosive is expressed as

$$P_{elec} = \sigma E^2 \Delta \, , \tag{1}$$

where σ is the electrical conductivity; Δ is the effective conduction zone width; and E is the applied electric field.

If the electrical power employed is large (~10^{15} W/m^2), the resulting improvements in explosive performance might be significant (*4*).

Demske (*5*) has shown that it is feasible to inject stored electrical energy into the conductive zone behind the dense detonation front of an explosive reaction. In his experiment, 108 kJ was stored in the capacitor bank, released, and transferred to a storage inductor. Upon initiation of the explosive, energy stored in the storage inductor is rapidly transferred through the electrodes and into the partially conductive zone behind the detonation front of an explosive reaction (as it propagates through the forward portion of the solid explosive). If the converted energy is redirected into the detonation zone towards the latter stages of its travel, an increase in detonation velocity to 10%–20% may be expected. Consequently, the pressure in the reaction zone is expected to increase by the order of 20%–40% (*5*). Thomas et al. (*6*) have also demonstrated that it is possible to couple energy from an external electrical source to gaseous plasma with increased efficiencies on the order of 10%. In their studies, detonation was initiated

in the driver by means of an exploding wire, which served as an initiator and as a means of varying the total driver energy during the tests. No detonation enhancement was achieved by ohmic heating prior to the C-J plane. Lee et al. (*7*) demonstrated the possibility of enhancing detonation properties by supplying electric energy into a detonating explosive. They observed an enhancement up to 3% of detonation velocity when electric energy equivalent to ~5% of the explosive chemical energy was supplied. Hence, energy coupling could be used as a technique of enhancing detonation properties.

2. Objective

The objective of this research effort is to assess the possibility of using electromagnetic fields to enhance the detonation velocity of explosives. It is anticipated that the introduction of high currents will increase the energy content of the conduction gases in the vicinity of the detonation front through ohmic heating. This increased energy should then lead to an increase in the detonation velocity.

3. Basic Technical Approach

In earlier experiments (*4*, *5*), the electric current was delivered to the detonation region by two parallel rails that were separated by a sheet of explosive as seen in figure 1. After the explosive was initiated at the left side of the rails, the electrical current from the power supply would flow along the top rail from the right end, down across the rails and back to the power supply along the bottom rail to the right end. The magnetic field generated by this current path is at the front of the detonation wave. As shown in figure 1, as the detonation region enters the magnetic field in the direction (v), the current crossing the rails feels a Lorentz force (F), which directs it away from the detonation region. It was presumed that because the reacted gas has a low electrical conductivity, the current would follow the detonation region but at some distance behind it. The Lorentz force, however, may be sufficient to force the current too far behind to be efficiently coupled to the detonation region, even though this current path may have an even lower electrical conductivity.

Thus, it is proposed to reproduce these earlier experiments, with the exception that the current will enter and leave the rails from the same end that the explosive is initiated, the left end in figure 2, which was the same setup by Thomas et al. (*6*) in their experiments with the detonation velocities of explosive gas mixtures. Because the magnetic field will subsequently be in the reacted gas region behind the detonation front, the Lorentz force (F) shall consequently be applied in the same direction (v) in figure 2, which will force the current toward the front. This

arrangement should improve the coupling of the electrical energy to the detonation region. Because the Lorentz force is dependent on the square of the current and the fact that explosive gas mixtures have a lower breakdown voltage than a solid explosive, Thomas et al. experiments may have been limited on the amount of electrical energy that could be delivered to the detonation front.

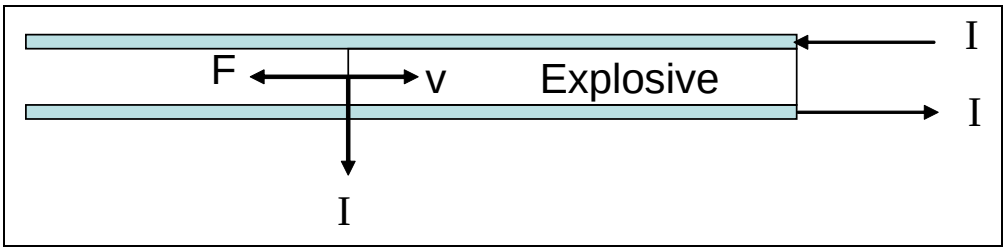

Figure 1. Schematic of (v) the travel direction of the detonation region, (F) the direction of the Lorentz force, and (I) the current path when the power supply is connected to the right end of the rails.

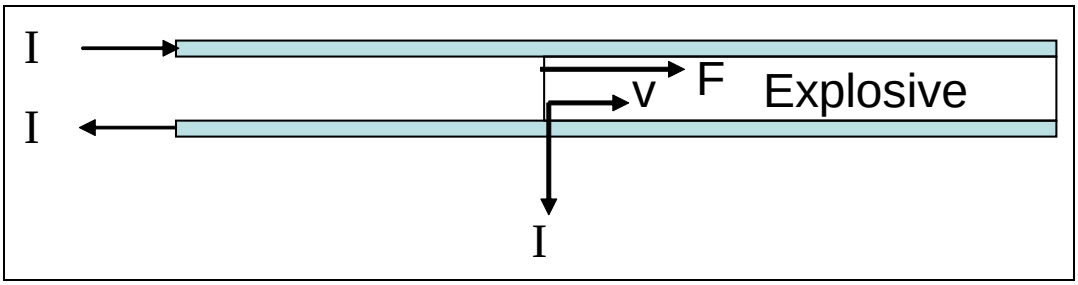

Figure 2. Schematic of (v) the travel direction of the detonation region (F) the direction of the Lorentz force, and (I) the current path when the power supply is connected to the left end of the rails.

In some experiments at the U.S. Army Research Laboratory (ARL), explosives were detonated in magnetic fields with no observable effects, but the effects may have been subtle. Therefore, it is proposed to use pulse power technology to produce a large magnetic field and study the effect of electromagnetic field coupling to an explosive.

The main problem is to devise a suitable method for introducing electrical current in the conductive gasses in the vicinity of a detonation front and using that current to modify the detonation rate. As of now, the magnitude of the magnetic field required to affect the various properties of the explosive is not known. Thus, the possible uses of a magnetic field to change the properties of the explosive, if any, are also not known. It is still a question whether the experimental design and subsequent tests will perform as predicted until the experiments are carried out. No numerical models or theories are readily available that predict the effects of an external electrical current or a magnetic field on the detonation wave of explosives.

The first step in this effort is to design an experimental setup where the electrical energy can be efficiently delivered to the advancing detonation region. An electrical pulsed power supply was designed and built at ARL that can deliver sufficient energy to the detonation region in a very short time. This new experimental arrangement required a design of the rails that maintains current conductivity during the detonation, and a power supply design that delivers the current to the rails in the very short time of the experiment. A series of tests using a well characterized rubberized flexible sheet explosive of Primasheet-1000 was conducted, where the detonation front velocity was measured at various electrical energies.

4. Experimental Setup

4.1 Current Pulse Power Supply

Figure 3 is the schematic of the power supply that was used in the experiment. The Pearson coil in this figure monitored the current as a function of time. A sample of a current trace for one experiment is shown in figure 4, where the explosive was 3 mm of Primasheet-1000 and the capacitor was charged to 5.5 kV. The period from 0 to 650 μs in figure 4 is when the energy that is stored in the capacitor is transferred to the 22-μH coil. At 0 μs, the 10.3-mF capacitor has charge that was deposited into it by a high-voltage supply (not shown in figure 3). When a light pulse is sent to the thyristor, the state of the thyristor changes from a non-conducting state to a conducting state. This allows current to flow through the 22-μH coil, the explosively opening switch (EOS) (described in section 4.2), and the Pearson coil, which monitors the current and back to the capacitor. Since the circuit at this time has an inductor L (the 22-μH coil), a resistor R (the sum of the coils resistance, the wires, the thyristor, plus the internal resistance of the capacitor) and a capacitor C (the 10.3-mF capacitor) all connected in series, it is known as an "LRC series circuit." Current in this type of circuit increases as a sinusoid to a maximum current as shown in figure 4, when the voltage on the capacitor is zero and the energy initially stored in the capacitor is now stored in the magnetic field of the coil. If there was no crowbar diode and no resistance in the circuit, all the energy of the magnetic field will be transferred back to the capacitor charging it to the opposite of its initial voltage. This transfer of energy between the capacitor and the inductor will continue indefinitely as a sine wave at some frequency. If there was some resistance in the circuit, then the amplitude of this sine wave will exponentially decay in time.

The crowbar diode, however, prevents this oscillation from occurring. When the current reaches the maximum at about 650 μs in figure 4, the voltage across the capacitor, the crowbar diode, and the inductor is close to zero, but it soon becomes negative afterwards. This reverse in voltage causes the crowbar diode to become forward biased and conduct the current out of the coil. This prevents the energy of the magnetic field from being transferred back into the

capacitor. Thus, the diode acts as if some conducting element, such as an iron crowbar, was suddenly thrown onto the circuit. If there were no resistance in the diode and the coil, this current would be constant forever; because there is no way that this energy can be dissipated. Indeed, this method is used in super conducting magnets, except that semi-conducting diodes are not used as crowbars. Since the circuit has resistance, however, the energy of the magnetic field can be dissipated as heat, and the current decreases. The rate that the current decreases at any time is where $R(t)$ is the total resistance of the circuit. The inductance of the circuit $L'(t)$

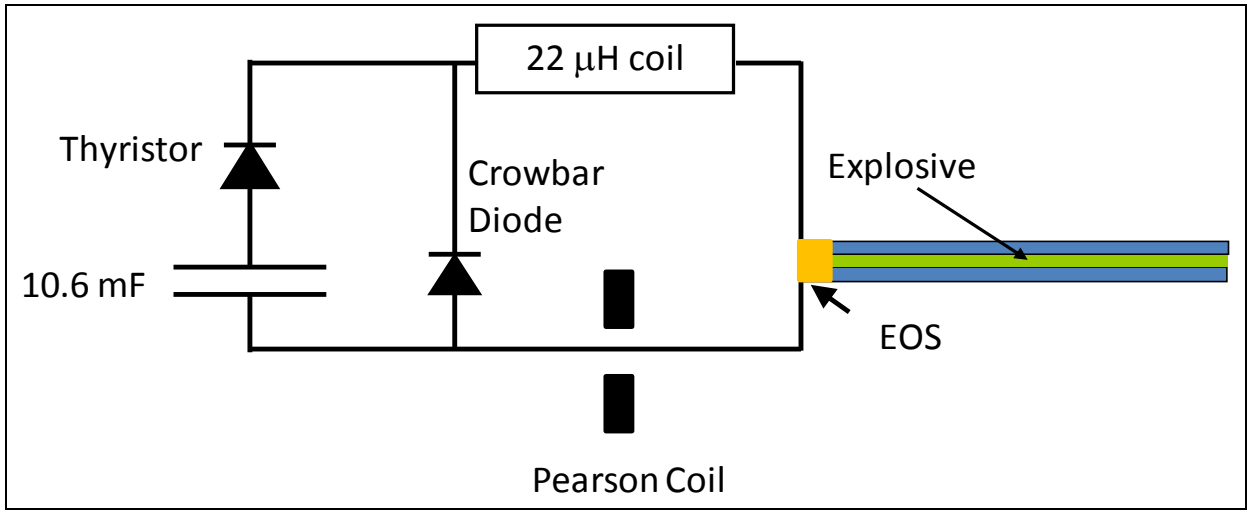

Figure 3. Schematic of the power supply.

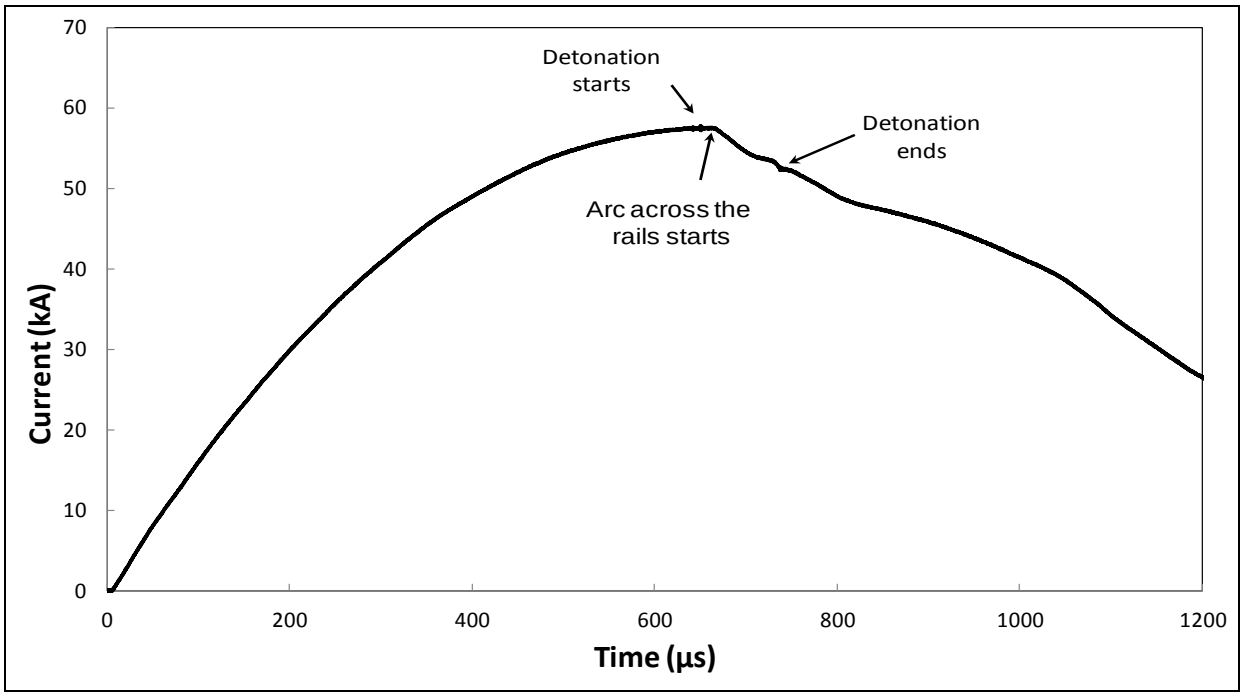

Figure 4. A typical current trace obtained during a test for Primasheet-1000.

$$I'(t) = -\frac{\left(R(t) + L'(t)\right) * I(t)}{L(t)}, \tag{2}$$

changes in this experiment, because the current path down the rails and across the detonation front changes with time. This change in inductance is small compared to the inductance of the 22-μH coil and can be usually ignored.

4.2 Explosively Opening Switch (EOS)

The Explosively Opening Switch (EOS) is a 25-mm-wide copper foil that is soldered onto the sides of the top and bottom rail as shown in figure 5. The sheet of the explosive being tested is extended beyond the end of the rails and sandwiched with a booster charge that is not shown in figure 5. When the booster charge detonates the sheet explosive, the sheet explosive then breaks the copper foil that is carrying the current to the coil. Once this current path is broken, the current must find another path, which is now across the detonation front.

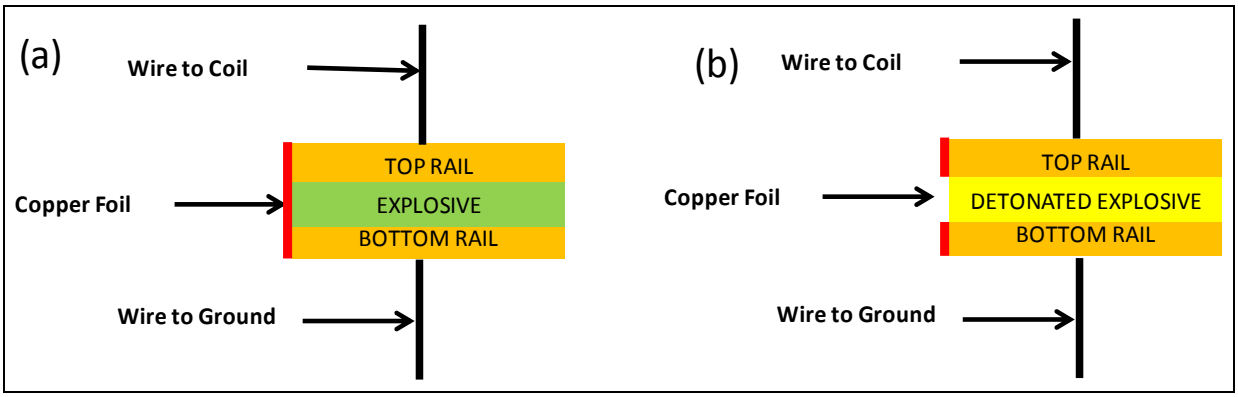

Figure 5. The EOS (a) before it is opened and (b) after it is opened.

4.3 Experimental Arrangement

All experiments were conducted at an indoor facility. The actual experimental arrangement is shown in figure 6. Figure 7 illustrates the high-voltage power supply enclosed in a wooden box.

Figure 6. Experimental arrangement (a) outside the blast chamber and (b) inside the blast chamber.

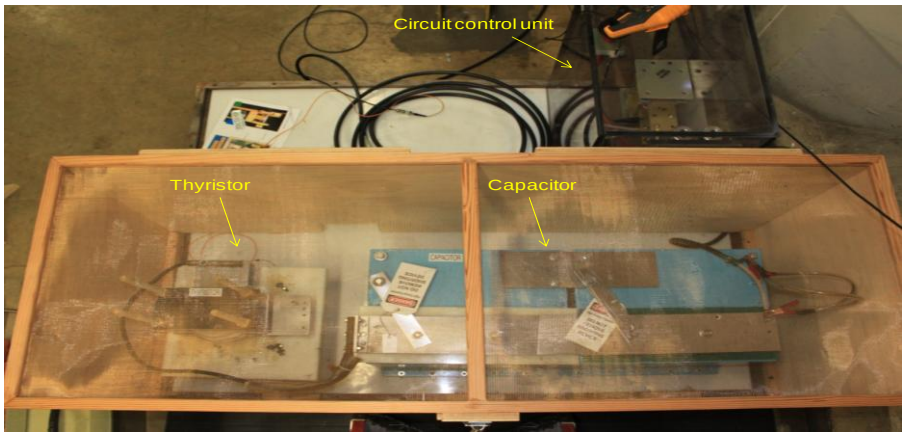

Figure 7. High-voltage power supply.

The experimental arrangement of electromagnetic coupling with explosive rails shown in figure 8 includes two copper plates separated by a 0.3-cm layer of Primasheet-1000 explosive. The plates are 2.54 cm wide × 50 cm long × 1.27 cm thick and 55 kJ of energy is transferred from a capacitor to a 22-μH inductor. When the detonation front comes between the copper plates, an EOS is ruptured and the energy stored in the inductor is rapidly transferred through the copper plates and into the conducting reaction zone of the detonation front.

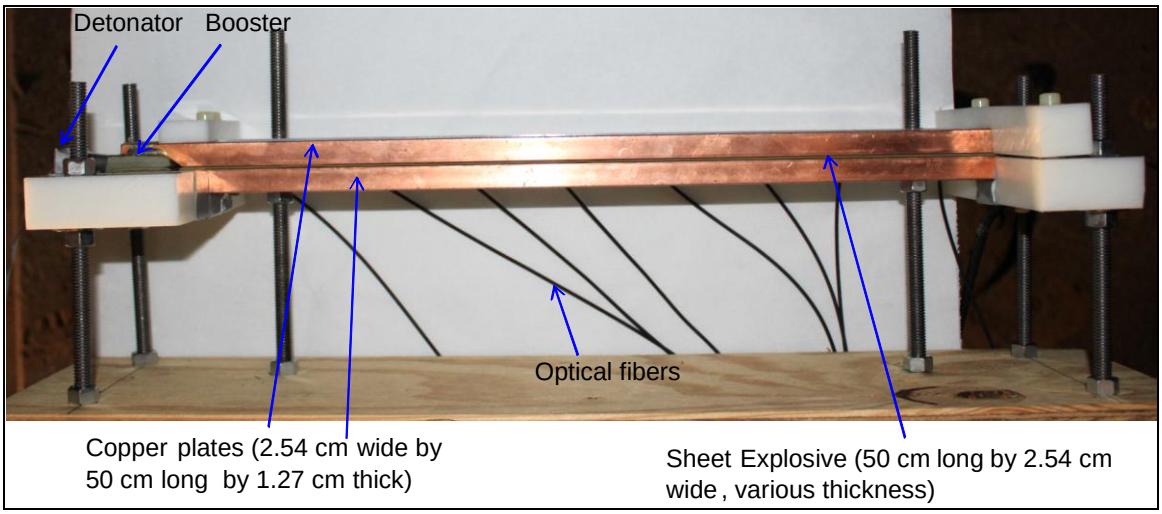

Figure 8. Electromagnetic coupling with explosive rails.

4.4 Diagnostic Techniques

4.4.1 Optical Fiber System to Determine the Detonation Velocity

An optical fiber system (shown in figure 9) was designed and built in house to determine the detonation velocity of Primasheet-1000 in highly electrically charged environments. Eight Optimate plastic optical fibers (1-mm core diameter, 2.2-mm fiber jacket, Part No. 501232-5, APM Inc., Harrisburg, PA) were cleaved and stripped back ~2 mm. The straight edge of the fiber was mounted near the explosive being tested without having to be polished. There was a controlled air gap created between the surface of the explosive and the cleaved end of the fiber to increase the light received from an explosion event. The fibers were evenly spaced 19.05 mm along the axis of the charge (figure 9a). A piece of paper was placed between the fiber and the surface of the explosive to create an air gap of ~0.17 mm (figure 9b). The shock heating of the air gap provides the bright light required for the measurement. Light entering the optical fiber probe was transported through the fiber to a control room outside of the blast chamber (the fiber length ~20 ft). In the control room, light from the fiber was connected (SMA union) to a high-speed DET10A-Si Biased photodetector (200- to 1100-nm wavelength, 1-ns rise time, Thorlabs, Newton, NJ). Using the time of arrival for the evenly spaced fibers, captured by an oscilloscope, the incremental detonation velocities were determined. After each test, several feet of each fiber were damaged. The fibers were then trimmed, cleaved, visually inspected by passing light through the fibers, and reused for the next experiments.

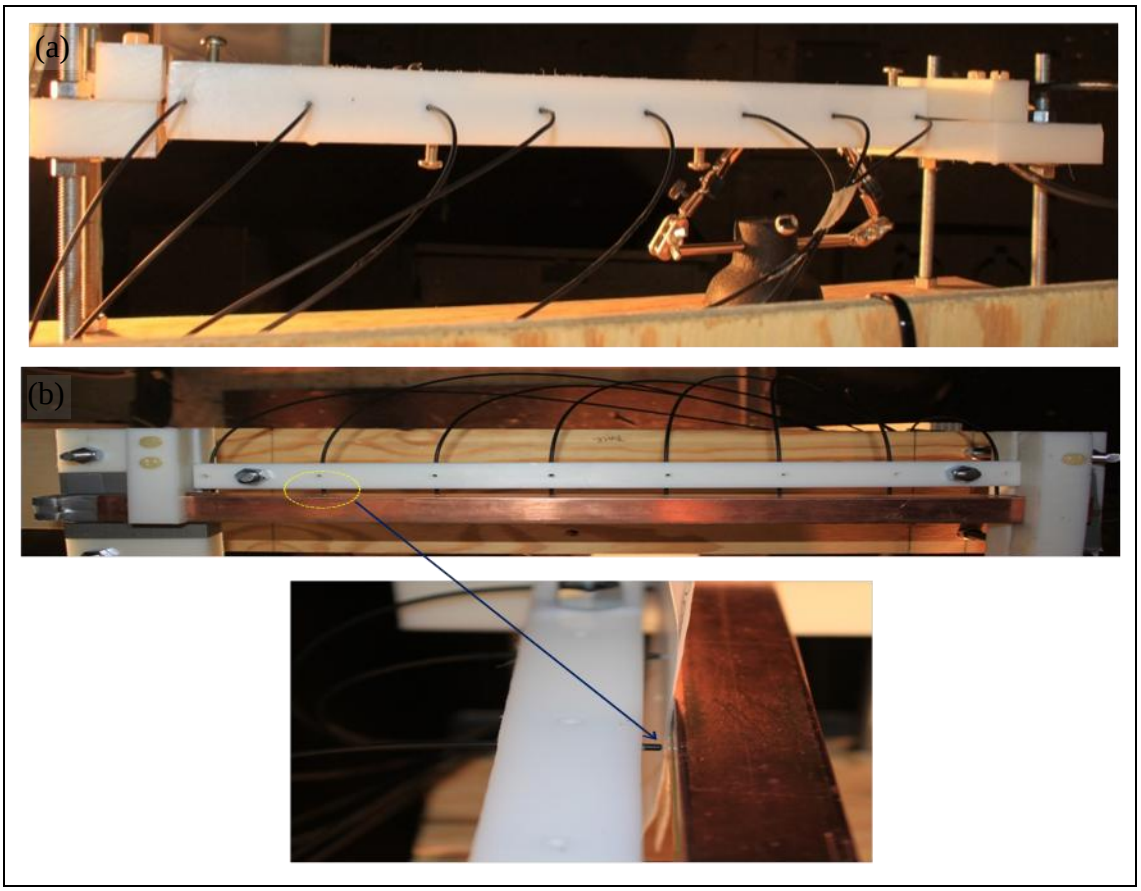

Figure 9. Eight-channel optical fiber system: (a) side and (b) top view.

4.4.2 High-Speed Imaging Techniques to Image the Advancing Detonation Front and Measure Detonation Velocity

The Cordin Model 132B Synchronous streak camera (Cordin Company, Salt Lake City, UT) was used to record the detonation front. The streak camera has a slit width of 0.6 mm and a maximum writing speed up to 20 mm/μs. Distance was recorded vertically and time was recorded horizontally (see figure 13). Streak records were analyzed on a vertical beam optical comparator (S-T Industries, Inc. Model 4600) with 20× objective lens. For each streak record, the track was read from the original position (distance vs. time) and slopes were recorded. The distance, time, and slope were recorded in order to calculate the detonation velocity. The detonation velocity was determined as follows:

$$\begin{aligned} \text{Detonation Velocity} &= \text{Scale Factor} * \text{Writing Speed of Camera} * \text{Tangent of the Angle} \\ &= \text{Scale Factor} * (4000 / \text{Camera Period}) * \text{Tangent of the Angle} \end{aligned} \quad (3)$$

In addition, the high-speed video camera images were captured with a resolution of 512 × 128 pixels using Photron FASTCAM SA5 high-speed camera (Photron USA, Inc., San Diego, CA). The camera frame rate was 100,000 frames per second with an exposure time of 370 ns. Figure 10 shows the experimental setup of the Cordin streak camera and the high-speed imaging Photron SA5 camera.

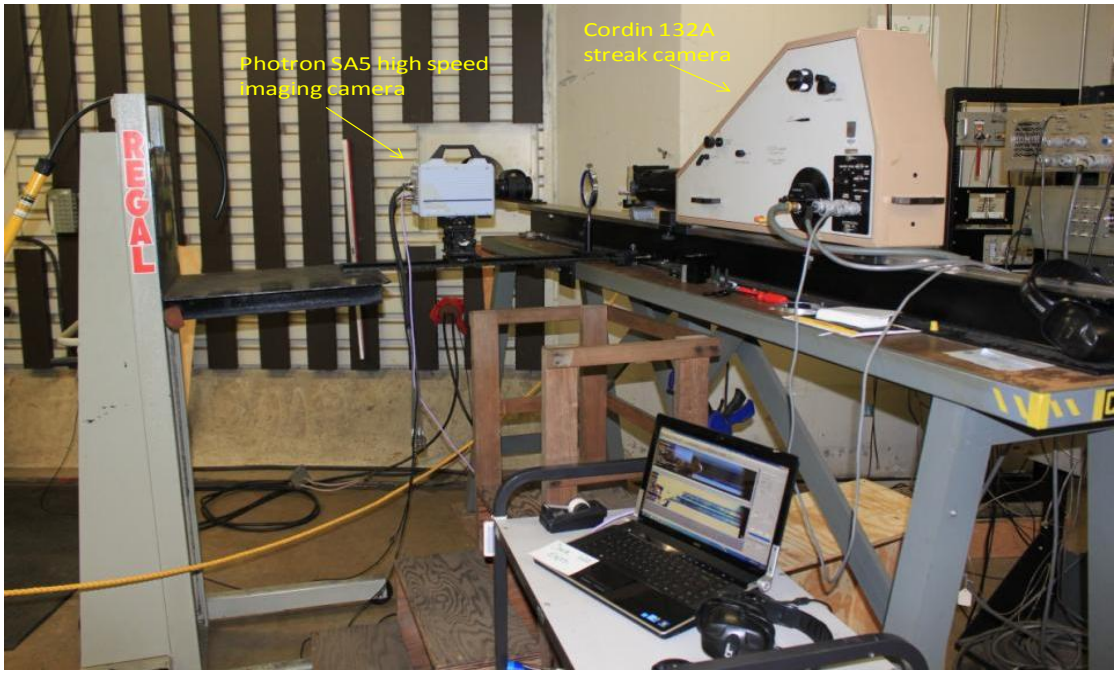

Figure 10. High-speed imaging experimental setup.

5. Results

5.1 High-Speed Imaging Record

Figure 11 shows a series of high-speed digital images following initiation of 1-mm-thick Primasheet-1000 without high-voltage electrical input. Figure 12 shows a series of high-speed digital images of 1-mm-thick Primasheet-1000 with high-voltage electrical input.

Figures 11(a) and 12(a) show an initial flash from the onset of detonation. As shown in figure 12(c) and 12(d), the upper edge and lower edge of the Primasheet-1000 show a brighter leading luminous trace compared to the leading edges of Primasheet-1000 in figure 11(c) and 11(d) when there was no high-voltage electrical input. It is presumed that the luminosity happened due to the jetting of the shockwave along the explosive/copper interface rather than a high-voltage discharge spark. The random nature of this phenomenon contributes to errors in analyzing the streak camera records for deriving the detonation velocity.

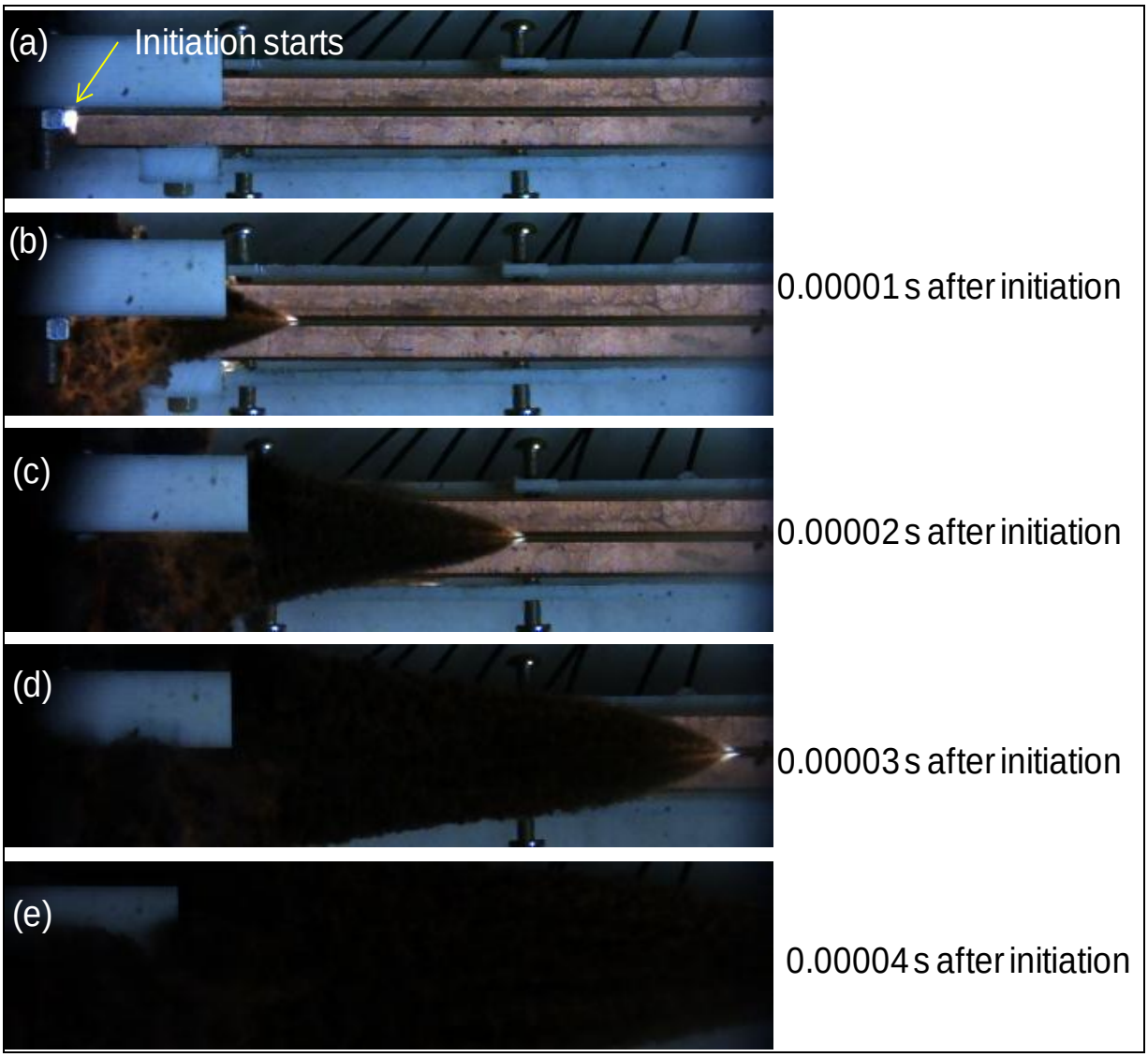

Figure 11. High-speed digital images following initiation of 1-mm-thick Primasheet-100 without high-voltage electrical input.

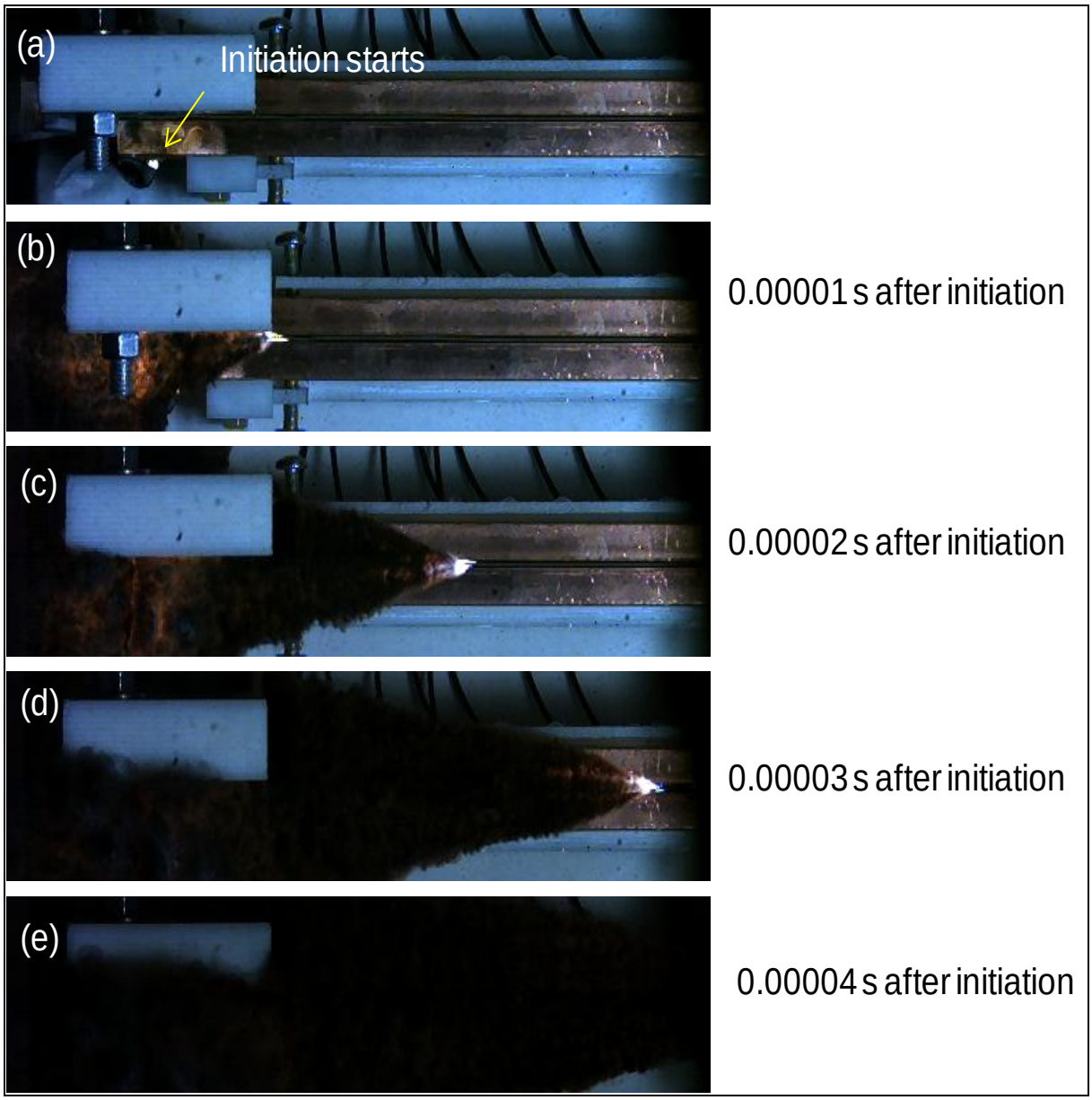

Figure 12. High-speed digital images following initiation of 1-mm-thick Primasheet-100 with 160.33-kJ electrical input.

5.2. Detonation Velocity Measurement

Figure 13 shows a typical streak camera record in which the maximum available energy in the circuit is deposited in the explosive. The reference detonation velocity was measured for each different explosive thickness, testing in the same setup only without supplying electric energy.

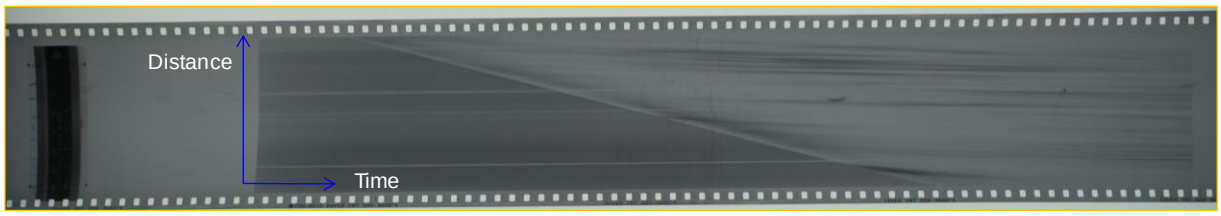

Figure 13. A typical streak record with an electric energy input of 160.33 kJ.

A velocity increase determined from the fiber optic records was ~4.1% for 1-mm-thick Primasheet-1000 and 1.2% for 2-mm-thick Primasheet-1000. On the other hand, the velocity increase rate from the streak camera records was determined to be ~3.4% for 1-mm-thick Primasheet-1000 and 2.7% for 2-mm-thick Primasheet-1000 (shown in table 1). The reported percent of velocity increase is the best estimate for the detonation velocity enhancement. With the 95% confidence, the true value lies within ±0.04% of the reported values. It is noted that the energy input is the energy stored in the capacitor, not the energy delivered to the explosive.

Table 1. Detonation velocity of Primasheet-100 without (w/o) and with (w/) high-voltage electrical input.

Explosive Thickness (mm)	**Detonation Velocity Measured From Streak Camera Record 95% Confidence Intervals (mm/μs)**			**Detonation Velocity Measured From Streak Camera Record 95% Confidence Intervals (mm/μs)**			**Energy Input (kJ)**
	W/O HV	**W/HV**	**Enhancement (%)**	**W/O HV**	**W/HV**	**Enhancement (%)**	
1	6.90	7.14 (±0.26)	3.4 (±0.04)	6.90	7.19 (±0.25)	4.1 (±0.04)	160.33 at 5.5kV
2	6.87	7.05 (±0.35)	2.7 (±0.05)	6.92	7.00 (±0.25)	1.2	160.33 at 5.5kV
3	6.99	6.91 (±1.02)	—	—	7.00 (±0.25)	—	160.33 at 5.5kV

Figure 14 is the section of the current traces in figure 15 between 600 and 780 μs. In this figure, there is a small noise pulse at 650 μs when the detonation circuit delivered a current pulse to the blasting cap. The slope of the current doesn't change, indicating that the resistance of the circuit has not changed. This is the time when the blasting cap is detonating a booster charge and when the 25-mm-wide EOS is being opened by the explosive between the rails. The slope of the current does noticeably change at about 667 μs, indicating that the resistance of the circuit has increased. This additional resistance is due to the detonation front between the rails, which lasts until about 734 μs when there is a small noise pulse and a change in the slope of the current. When the detonation front reaches the end of the rails, there is still about 30.3 kJ of energy left in the inductor that must be dissipated by forming a discharge arc through the air that has a larger resistance. Given the detonation velocity of 7 mm/μs that was measured by the streak camera and the light pipe data, the time for the detonation front to travel the length of the rails, 508 mm, is about 73 μs. Subtracting this time from the 734 μs, the time that the detonation front should start at about 661 μs, which is consistent with the change in the slope at about 667 μs.

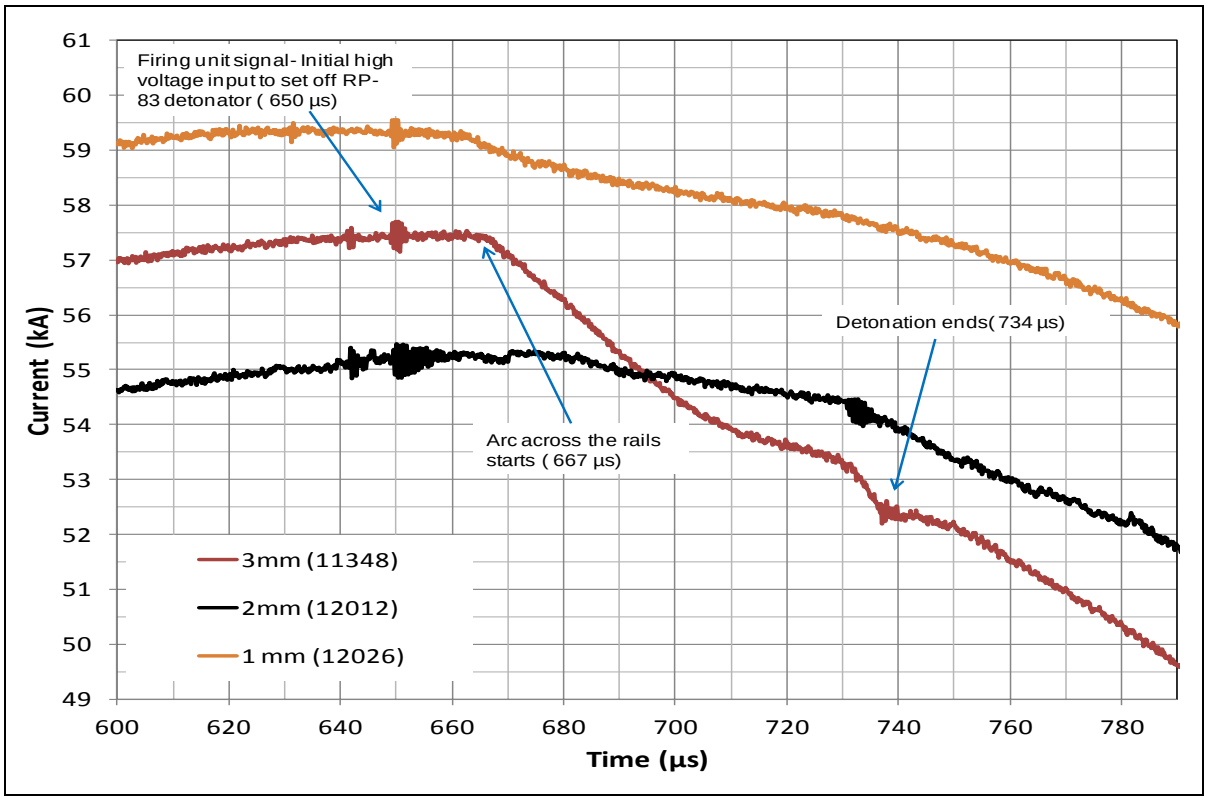

Figure 14. Current traces during the detonation of the 1-, 2-, and 3-mm-thick Primasheet-1000.

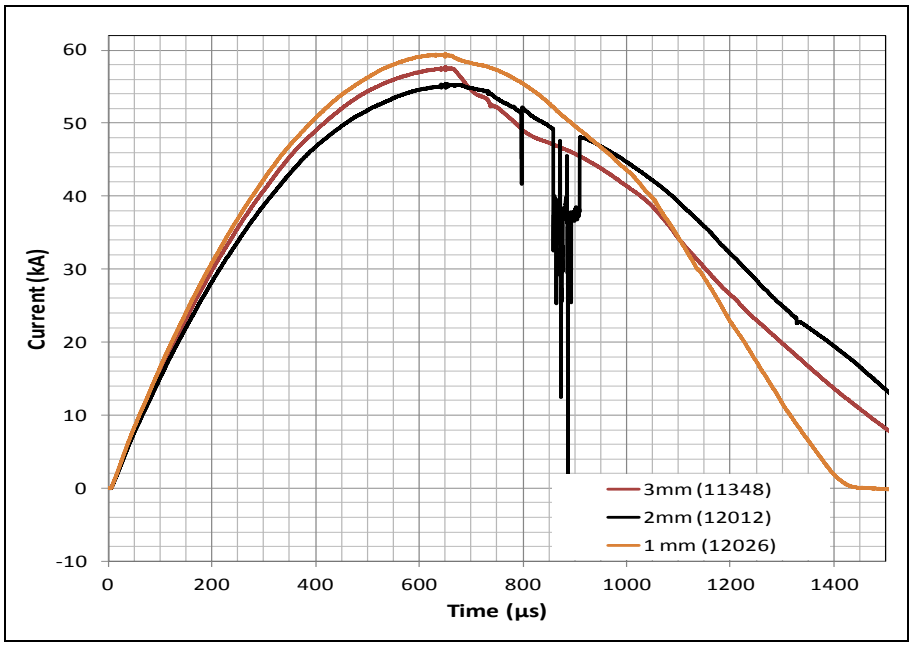

Figure 15. Current traces during tests for 1-, 2-, and 3-mm-thick Primasheet-1000.

It is postulated that having the direction of the J × B force in the same direction as the direction of the detonation wave will improve the coupling of the current with the detonation front. To test this hypothesis, several experiments were conducted using 1-mm-thick Primasheet-1000 where the directions of the J × B force and the detonation velocity were in opposite directions. This was accomplished by simply connecting the wire leads to the opposite ends of the rails in figure 3. The current traces for some of these experiments are shown in red in figure 16. The blue trace is for a test where the J × B force and the detonation velocity are in the same direction as a comparison. The upper red trace has some weak features and the decay of the current is slower than all the other traces after 750 µs. This may indicate that part of the current is being delivered to the detonation front, but the resulting arc may be spread out over a large area to have such a low resistance. The lack of features in the lower red trace may indicate that none of the current was coupled to the detonation front, and all of the current was flowing through an arc that stayed at the end of the rails. Thus having opposing directions of the J × B force and the detonation velocity may not exclude the current from being coupled to the detonation front, but this coupling may be unreliable.

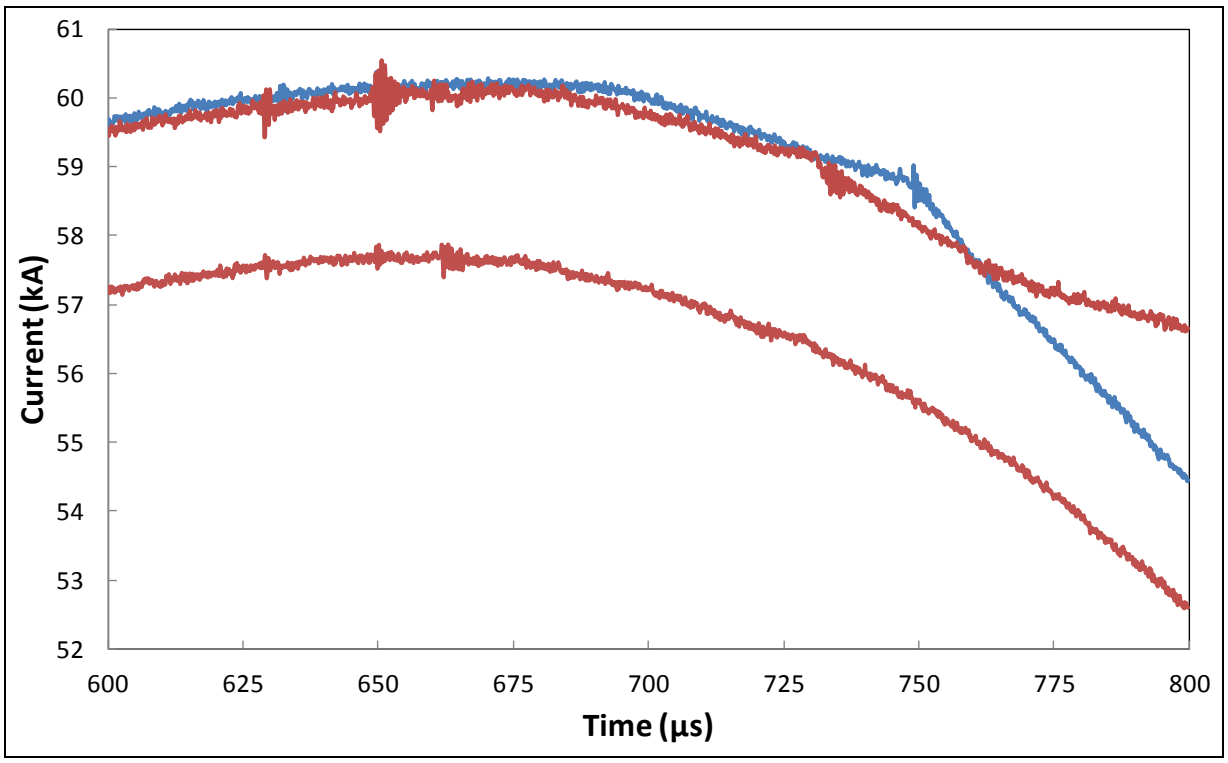

Figure 16. Current traces where the directions of the J × B force and the detonation velocity are in the opposite directions (red) and in the same direction (blue).

6. Conclusions

Initial results show that there was an increase of ~3.4%–4.1% (95% chance that true mean is likely to lie within this interval) in the detonation velocity observed in a 0.1-cm-thick layer of Primasheet-1000 while inputting the electric energy into the reaction zone. There was a 1.2%–2.7% (95% confidence interval) enhancement in the detonation velocity observed in a 0.2-cm-thick layer of Primasheet-1000. No detonation velocity enhancement was observed in 0.3-cm-thick layers of Primasheet-1000 explosive. It may be possible to use this electrical energy coupling technique to enhance detonation velocity of an explosive. Future works would be to measure the voltage wave forms, the breakdown voltage of the un-reacted Primasheet-1000, and the resistance of detonating Primasheet-1000. Further improvements in diagnostics are needed to obtain an accurate and reliable current data for analysis.

7. References

1. Weiser, V.; Kelzenberg, S.; Eisenreich, N. Influence of the Metal Particle Size on the Ignition of Energetic Materials. *Propellants, Explosives, Pyrotechnics* **2001**, *26*, 284–289.

2. Wilkinson, C. R.; Anderson, J. G. *An Introduction to Detonation and Blast to the Non-Specialist*; DSTO-TN-0526; Defence Science and Technology Organisation Systems Sciences Lab: Salisbury, Australia, 2003.

3. Cooper, P. Personal communication, May 2007.

4. Tasker, D. *The Properties of Condensed Explosives for Electromagnetic Energy Coupling*; NSWC TR 85-360; Naval Surface Weapons Center: Silver Spring, MD, October 1985.

5. Demske, D. *The Experimental Aspects of Coupling Electrical Energy Into a Dense Detonation Wave*: *Part 1*; NSWC TR 79-143; Naval Surface Weapons Center: Silver Spring, MD, May 1982.

6. Thomas, G.; Edwards, D.; Edwards, M.; Milne, A. Electrical Enhancement of Detonation. *J. Phys. D: Appl. Phys.* **1993**, *26*, 20–30.

7. Lee, J.; Kuk, J.; Kim, C.; Hwang, E. Enhancement of Detonation Properties by Electric Energy Input. *Proceedings of the American Institute of Physics Conference on Shock Compression of Condensed Matter*, Snowbird, UT, 28 June–2 July 1999; Vol. 505, pp 865–868.

INTENTIONALLY LEFT BLANK.

Appendix A. Detonation Velocity Log

Table A-1. Detonation velocity log.

Date	Shot No.	Material	Thickness	Charging Voltage	Streak (y/n)	Photron (y/n)	Fiber Optics	Detonation Velocity	
								Streak	Fibers
12/27/2011	1136-1	Prima Sheet	2 mm	NA	Y	Y	Y	6.87	6.92
12/7/2011	1134-1	Prima Sheet	2 mm	5.5KV	N	Y	N	—	—
12/8/2011	11342-1	Prima Sheet	2 mm	5.5KV	Y	Y	N	7.19	—
12/9/2011	11343-1	Prima Sheet	2 mm	5.5KV	Y	Y	Y	6.91	6.98
1/12/2011	12012-1	Prima Sheet	2 mm	5.5KV	Y	Y	Y	7.06	7.02
12/1/2011	11335-1	Prima Sheet	3 mm	NA	Y	Y	N	6.99	—
12/6/2011	11340-1	Prima Sheet	3 mm	5.5KV	Y	Y	N	6.99	—
12/14/2011	11348-1	Prima Sheet	3 mm	5.5KV	Y	Y	N	6.83	—
1/4/2012	12004-1	Prima Sheet	1 mm	NA	Y	Y	Y	6.9	6.9
1/6/2012	12006-1	Prima Sheet	1 mm	5.5KV	Y	Y	Y	7.25	7.29
1/18/2012	12018-1	Prima Sheet	1 mm	5.5KV	Y	Y	Y	7.05	7.02
1/24/2012	12024-1	Prima Sheet	1 mm	5.5KV	Y	Y	Y	6.83	7.35
1/26/2012	12026-1	Prima Sheet	1 mm	5.5KV	Y	Y	Y	7.11	7.08
2/1/2012	12032-1	Prima Sheet	1 mm	5.5KV	Y	Y	—	6.89	7.06
2/27/2012	12058-1	Prima Sheet	1 mm	5.5KV	Y	Y	Y	7.25	6.93

Appendix B. Fiber Optic Detonation Velocity Measurement Log

This appendix appears in its original form, without editorial change.

Primasheet 1 mm HV

Date	Test #	Charge #	Pin #	1	2	3	4	5	6	7	8	AVG
1/24/2012	12024-1	EMCE	Pin Distance (mm)	58.0568	58.0568	58.0568	58.0568		116.1100	58.0568	58.0568	
			TOA (µsec)	26.3580	34.6760	42.6048	50.5652		66.1088	73.9348	81.9916	
			ΔT	26.3580	8.3180	7.9288	7.9604		15.5436	7.8260	8.0568	
			V at pin	0.0000	6.9797	7.3223	7.2932	#DIV/0!	7.4700	7.4185	7.2059	7.2816

Primasheet 1 mm HV

Date	Test #	Charge #	Pin #	1	2	3	4	5	6	7	8	AVG
1/18/2012	12018-1	EMCE	Distance (m	58.06	58.06	58.06	58.06		116.11	58.06	58.06	
			TOA (µsec)	26.26	34.62	43.14	51.44		67.67	76.08	84.21	
			ΔT	26.26	8.35	8.52	8.30		16.23	8.41	8.13	
			V at pin	0.00	6.95	6.81	6.99	#DIV/0!	7.15	6.90	7.14	6.99

Primasheet 1 mm HV

Date	Test #	Charge #	Pin #	1	2	3	4	5	6	7	8	AVG
1/26/2012	12026-1	EMCE	Pin Distance (mm)	58.0568	58.0568	58.0568		116.1136	58.0568	58.0568	58.0568	
			TOA (µsec)	37.5752	45.9592	54.2908		70.5768	78.5044	86.9400	95.1468	
			ΔT	37.5752	8.3840	8.3316		16.2860	7.9276	8.4356	8.2068	
			V at pin	0.0000	6.9247	6.9683	#DIV/0!	7.1297	7.3234	6.8824	7.0742	7.0504

Primasheet 1 mm HV

Date	Test #	Charge #	Pin #	1	2	3	4	5	6	7	8	AVG
1/6/2012	12006-1	EMCE	Pin Distance (mm)	19.05	19.05	19.05	19.05	19.05	19.05	19.05	19.05	
			TOA (µsec)	37.75	40.32	43.06	45.63	48.37	50.89	53.33	56.08	
			ΔT	37.75	2.57	2.74	2.58	2.74	2.51	2.44	2.75	
			V at pin	0.00	7.42	6.96	7.40	6.95	7.58	7.79	6.94	7.29

Primasheet 1 mm W/O HV

Date	Test #	Charge #	Pin #	1	2	3	4	5	6	7	8	AVG
1/4/2012	12004-1	EMCE	Distance (r	19.05	19.05	19.05	19.05	19.05	19.05	19.05	19.05	
			TOA (µsec	38.68	41.28	44.00	46.76	49.46	52.43	55.05	57.98	
			ΔT	38.68	2.60	2.72	2.76	2.70	2.97	2.62	2.93	
			V at pin	0.00	7.34	6.99	6.91	7.07	6.41	7.26	6.50	6.93

Primasheet 2 mm W/O HV

Date	Test #	Charge #	Pin #	1	2	3	4	5	6	7	8	AVG
12/27/2011	113611	EMCE	Distance (r	25.4	25.4	25.4	25.4	25.4	25.4	25.4	25.4	
			TOA (µsec	42.38	46.08	49.89	53.57	56.90	60.62	64.55	68.14	
			ΔT	42.38	3.70	3.8148	3.6752	3.3356	3.724	3.9296	3.5888	
			V at pin	0.00	6.87	6.66	6.91	7.61	6.82	6.46	7.08	6.92

Primasheet 2 mm HV

Date	Test #	Charge #	Pin #	1	2	3	4	5	6	7	8	AVG
1/12/2012	12012-1	EMCE	Pin Distance (mm)	58.06	58.06	58.06	58.06	58.06	58.06	58.06	58.06	
			TOA (µsec)	27.17	35.51	43.76	51.95	60.27	68.58	76.69	85.11	
			ΔT	27.17	8.34	8.24	8.19	8.32	8.31	8.11	8.41	
			V at pin	0.00	6.96	7.04	7.09	6.98	6.98	7.16	6.90	7.02

Primasheet 1 mm HV

Date	Test #	Charge #	Pin #	1	2	3	4	5	6	7	8	AVG
2/1/2012	12032-1	EMCE	Pin Distance (mm)	58.0568	58.0568	58.0568	58.0568	58.0568	58.0568	58.0568	58.0568	
			TOA (µsec)	38.3128	46.8368	55.3324	63.3948	71.9920	79.9312	87.4732	96.2112	
			ΔT	38.3128	8.5240	8.4956	8.0624	8.5972	7.9392	7.5420	8.7380	
			V at pin	0.0000	6.8110	6.8337	7.2009	6.7530	7.3127	7.6978	6.6442	7.0362

NO. OF COPIES	ORGANIZATION
1 (PDF)	DEFENSE TECHNICAL INFORMATION CTR DTIC OCA
1 (PDF)	DIRECTOR US ARMY RESEARCH LAB RDRL CIO LL
1 (PDF)	GOVT PRINTG OFC A MALHOTRA
	ABERDEEN PROVING GROUND
1 (PDF)	RDRL WML C T PIEHLER

INTENTIONALLY LEFT BLANK.